VR-Learning System: Virtual Cooking Training System

Kohei Sato and Kenji Funahashi
Dept. of Computer Science and Eng., Nagoya Institute of Technology,
Gokiso-cho, Showa-ku, Nagoya 466-8555 Japan
Corresponding Author: ksato@center.nitech.ac.jp

ABSTRACT

There are many kinds of education. The method of education has been developed from oral communication and textbook to broadcasting into e-learning system with electric textbook on PC monitor. However it is usually difficult to have a good environment for experience at a self-learning situation and e-leaning systems. In this paper, we describe a cooking learning system using VR technology for beginners, as a VR-learning system. Using our system you can learn cooking anytime, anywhere, even if you have no time to learn cooking because of busyness. In addition, we define the all objects such as rice and a piece of foods as a group of individual bodies (GIB). We have proposed a manipulation model of the GIB which calculates the GIB behavior according to transform surface, and enables high speed interactive operation.

Keyword: VR-learning, Virtual cooking system, Interactive manipulation, A group of individual bodies, Transform surface

1. INTRODUCTION

There are many kinds of education, i.e., oral communication, self-education with textbook, educational program broadcasted on radio/TV, and e-learning recently. It is necessary to choose an appropriate method for your each purpose. The textbook can make you free from place like school, and the educational program liberate you also from time [NHK] [Hilliard] [Swan] (Fig.1, 2). The education method has changed recently, you can browse electric textbook on PC monitor, and of course watch and listen sound and video. You usually call this system as an e-learning [Garrison] [Marriott] (Fig.3). Some of systems can mark answer for questions, also voice which student vocalizes. However it is usually difficult to have a good environment for experience at a self-education situation and e-learning systems.

In our laboratory, we focus on experience-type learning system based on virtual reality technology, and are developing a VR cooking learning system for beginners [Morii2010] [Morii2011]. Arrangements, planning and procedure are very important on cooking, for example, main dish which gets cold soon have to be cooked last, stewed dish which takes some time have to be started to prepare, and an expert usually make a salad and wash cookware already used while boiling something. Using our system you can learn time management on cooking anytime,

Fig. 1: Radio text, English-conversation

Fig. 2: Education program on radio

anywhere, even if you must cook by yourself but you cannot go cooking school because of busyness. We are developing also VR chemical laboratory experience system (Fig.4) [Natsume][Tanabashi][Miyashita2011][Miyashita2012][Funahashi2000] [Funahashi2001][Uchiyama].

There is another research about learning and training related to cooking [Kato]. They try to represent a process to grill meat. A part of our developing system is focused on interaction of a gather of small bodies such as rice and a piece of foods, i.e., cooking fried rice. Researches about lava and sand are related to our research [Stora][Onoue]. However they calculate the behavior of all solid materials one by one, so the amount of calculation takes much time. They cannot be applied for an interactive system or cannot treat object globally.

In our idea, we treat the all objects which is in a cooking container such as frying pan, in other words, a gather of small bodies as one object. We define the object as a group of individual bodies (GIB). We have proposed a manipulation model of the GIB which calculates the GIB behavior according to the forces effected through a container, and enables high speed interactive operation [Ishihara][Kurimoto]. In this model, a GIB is not represented with a gather of individual particles but a height field which is defined on the bottom surface of a container. We enable to represent natural behavior that user expect (Fig.5).

In this paper, we describe GIB manipulation model with spatula-formed cook-

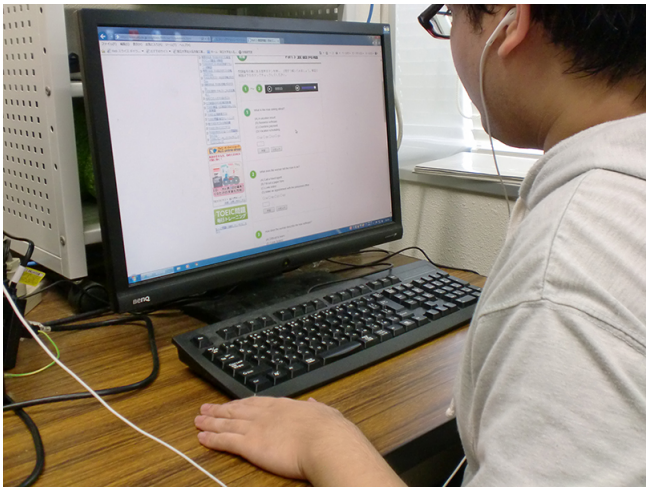

Fig. 3: Self-study using e-learning system

ware which user can operate freely on VR cooking system, especially pressing and scooping operations. This manipulation has difficult problems and we assume that the operating surface of a spatula is vertical or horizontal. In chapter 2 we explain the manipulation model of a GIB that we have proposed. In chapter 3 we propose GIB operations with spatula-formed cookware. Then chapter 4 shows experiments and results of the proposed system.

Fig. 4: Chemical lab experience system

2. MANIPULATION MODEL OF GIB

2-1. Container and transform surface

In this model, we treat the GIB existing in one cooking container as one operation object even if it is divided into multiple in an appearance. First we define the cooking container as below.

- Bottom of container: Plane figure of convex polygon
- Side of container: Vertical to the bottom

Fig. 5: VR cooking learning system

In addition, a GIB is defined as a height field which is fixed on the container bottom (Fig.6). When the volume of a part of GIB on the grid (x, y) is defined as $V(x, y)$, the GIB volume V_c on the container is calculated as below.

$$V_c = \sum V(x, y) \tag{1}$$

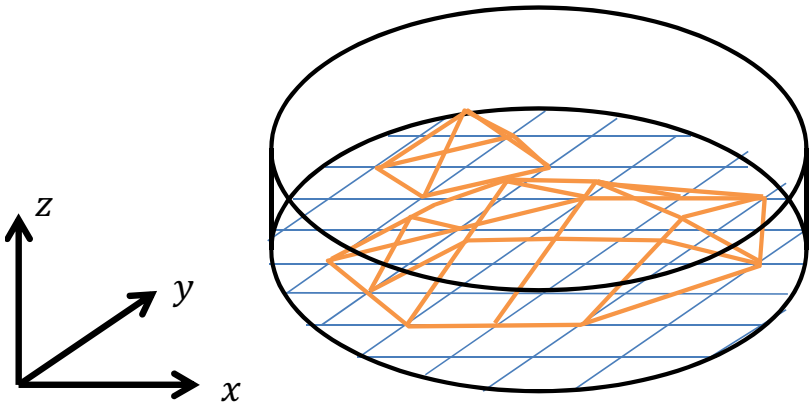

Fig. 6: GIB on a Container

The behavior of the GIB is represented by varying the height of each grid in each time appropriately. In particular, we represent the variation of the GIB behavior in a curved surface which is called Transformation Surface (TS). For example, when a GIB exists in the container (Fig.7-1), it is expected to slide down to the lower part of the container according to gravity. Then, the TS is applied around the GIB (Fig. 7-2). As a result the GIB is moved (Fig.7-3).
Actually GIB behavior is complex, so it is difficult to calculate the shape of TS. Thus, we use an alternative process. We think a GIB on the bottom receives constant forces from gravity, friction and reaction form the container. Therefore, we use a TS of a half of elliptic cylinder shape to simplify calculation (Fig.8).

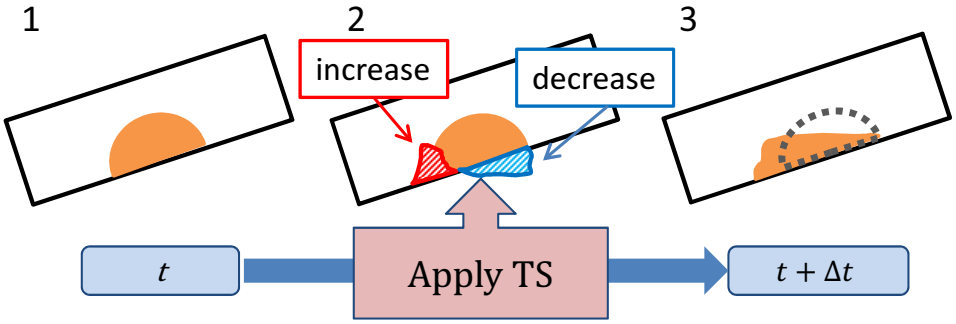

Fig. 7: Vertical section of GIB in cylinder container

Parameters of the TS are defined as below (Fig.9). The size of the TS is determined from the semi major axis of elliptic a and the semi minor axis of elliptic b. The place and the direction of the TS depend on the center of TS o_D and the center axis L_D. The length of a is calculated from the volume of the GIB V_c and reaction force form the side F_N. The length of b is calculated from V_c, the appropriate force that the GIB is received F_b, a static friction force from the bottom μ, and a dynamic one μ'. The coordinate of o_D is determined from a, the center of the GIB G_c, and the direction of F_b. These parameters are calculated as below.

$$a = \begin{cases} T_1 - |F'_N| & (T_1 \geq |F'_N|) \\ 0 & (T_1 < |F'_N|) \end{cases} \tag{2}$$

$$b = \begin{cases} (|F_b| - \mu')T_2\sqrt{V_c} & (|F_b| \geq \mu) \\ 0 & (|F_b| < \mu) \end{cases} \tag{3}$$

$$o_D = G_c + \frac{F_b}{|F_b|}a \tag{4}$$

The TS can represent a difference of properties of the GIB such as viscosity by changing constants T_1, T_2. The axis L_D is perpendicular to the direction of F_b, passing on o_D. The length of r_D is appropriate constant which is longer than the radius of container bottom.

Using the TS, a GIB on a tilted container changes its shape to represent motion (Fig.10). To increase volume of GIB at lower part, a half of elliptic cylinder TS is applied at the appropriate place (Fig.10-2). Then the volume of the TS is added to the volume of the GIB (Fig.10-3). Later, the volume of the GIB is corrected (Fig.10-4). Finally, the GIB moves.

2-2. Shake GIB manipulation

A GIB in a container also should be transformed by shaking a container. However, we have determined the position of a TS depending on the angle of the container, in other words the gravity force. Consequently we regard the shape variation of a GIB by shaking a container in the same light as one by tilting a container (Fig.11). When a container is accelerated by the acceleration a, we consider that a GIB in

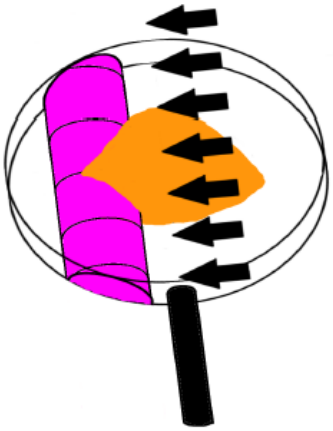

Fig. 8: TS applied on cylinder container

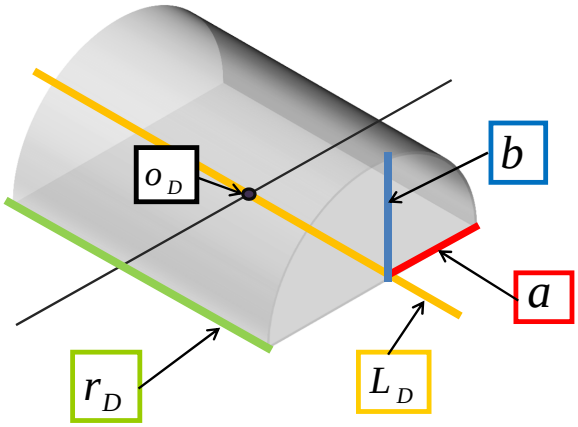

Fig. 9: Half of elliptic cylinder TS

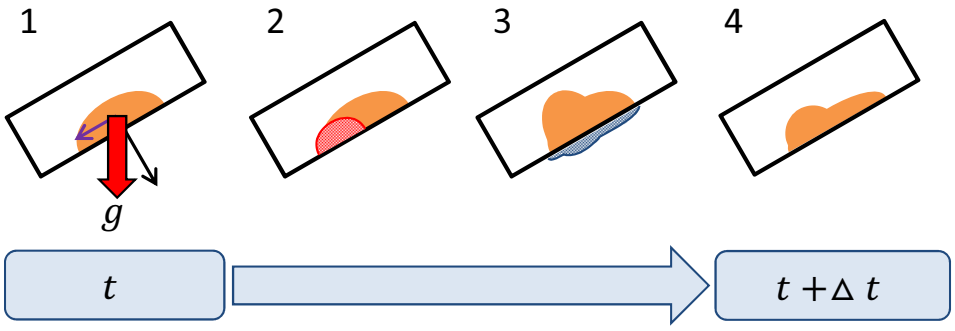

Fig. 10: Alternative process

a container receives a reaction force by the acceleration $-a$, and we apply a TS according to the resultant force g' as relative gravity (Fig.12). Then we proceed shake manipulation according to the same process of tilting manipulation.

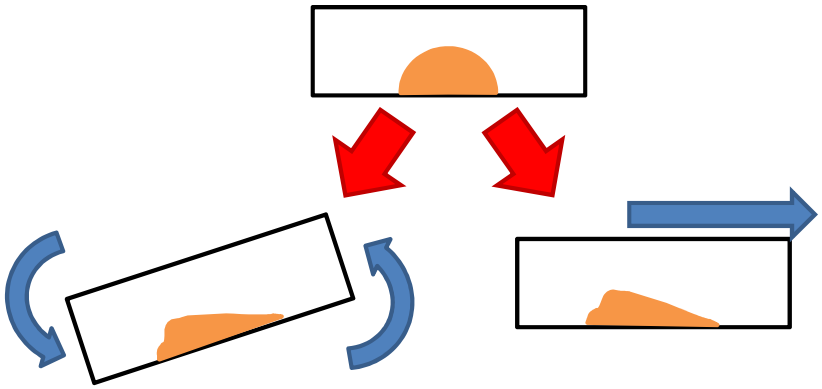

Fig. 11: Tilt operation and accelerated translation

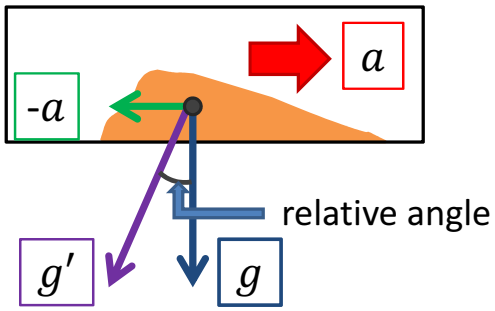

Fig. 12: Relative angle for container acceleration

2-3. Toss GIB manipulation

In this model, we represent the toss GIB manipulation which we swing up a pan and rise up pieces of ingredients in container into the air. This toss manipulation is used for the purposes of mixing ingredients, adjusting temperature, and extracting water. However it is difficult to define the height field of GIB the bottom of a partial sphere container like a Chinese pan, so we introduce the container height field to represent the shape of container (Fig.13). The height of the container from the height field face $h_s(x_i, y_j)$ on the grid (x_i, y_j) is calculated by the radius of the partial sphere R_s as below.

$$h_s(x_i, y_j) = R_s - \sqrt{R_s^2 - (x_i^2 + y_i^2)} \tag{5}$$

In the model using a partial sphere container, we apply a half of spheroid TS to the appropriate position depending on the influence of gravity and the convex bottom of the container. We represent a slide GIB manipulation by gravity on a

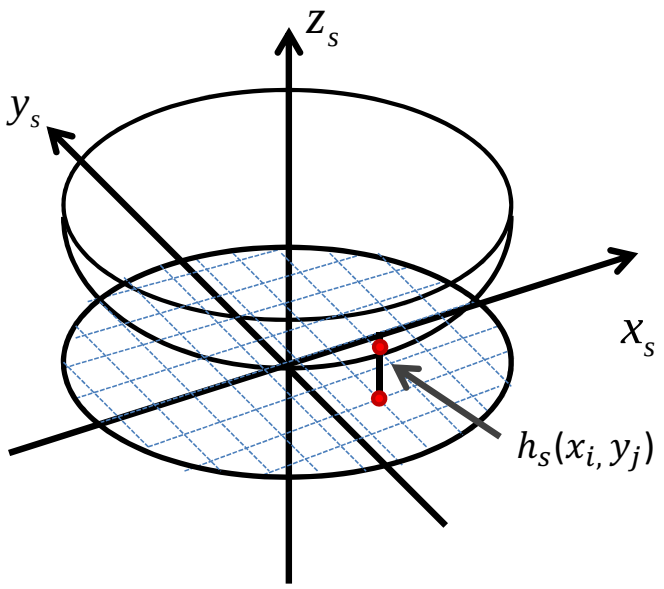

Fig. 13: Height field for partial sphere container

partial sphere container to apply a TS similarly in order to maintain the rate of the height of each grid.

When we shake a container aggressively such as a toss manipulation, a GIB receives force from a partial sphere container by changing the dynamic position. We determine whether a GIB slides up or down on the container based on the direction of the force, and we represent an slide GIB manipulation to any direction applying a TS as same as the slide manipulation by gravity. In addition, when a toss of a GIB happens because a GIB slides up, it is necessary to convert a GIB expressed in a height field into particles in the air. We call these particles as GIB particles. The GIB particles are small solids gathered only in volume V_s, and they fall freely according to gravity. We also determine the volume of conversion to particles by force that a GIB receives from a container, though the parameters are determined empirically. When the number of k GIB particles are generated and the number of l GIB particles are received in a container at time t, the volume of the GIB in the container V is calculated as below, and we represent a toss GIB manipulation.

$$V(t) = V(t - \Delta t) - kV_s + lV_s \tag{6}$$

2-4. Probability particle and free fall particle

The minimum component of GIB in real world is a small solid, and it has a finite size. However the GIB in a cooking container is represented with a height field, so it is not define the minimum component. Therefore, the minimum component of GIB which is represented with a height field is defined as α, and we draw the only GIB of the size that is higher than the minimum component α. If a height of a grid $f(x_i, y_j) < \alpha$ exists, the existence of GIB in the grid is judged statistically using $f(x_i, y_j)$, and we draw the GIB according to the result. We define another

height field to draw the GIB which existence is determined statistically. The value of each gird in the drawing height field $f^e(x_i, y_j)$ is calculated as below according to the height field defined in a cooking container.

- if $f^e(x_i, y_j) < \alpha$

$$f^e(x_i, y_j) = \begin{cases} (P(x_i, y_j)) & 0 \\ (1 - P(x_i, y_j)) & \alpha \end{cases} \tag{7}$$

- if $f^e(x_i, y_j) \geq \alpha$

$$f^e(x_i, y_j) = f(x_i, y_j) \tag{8}$$

Where $P(x_i, y_j)$ is the propability which the GIB exists in the grid (x_i, y_j), and it is calculated as below.

$$P(x_i, y_j) = \frac{f(x_i, y_j)}{\alpha} \tag{9}$$

In addition, we represent that GIB falls out from container with particle which suppressed computational cost. Fig.14 shows the boundary if particles spill out from container. The boundary A is for tilting operation, and the boundary B is for pushing operation with cookware such as spatula to calculate simply. Besides, θ is the angle that a piled up GIB keeps stability without collapsing voluntarily. If a height of GIB exceeds either of the two boundaries, we represent the spill manipulation by converting the particle based on the existence probability into the free fall particle, and dropping into outside of container.

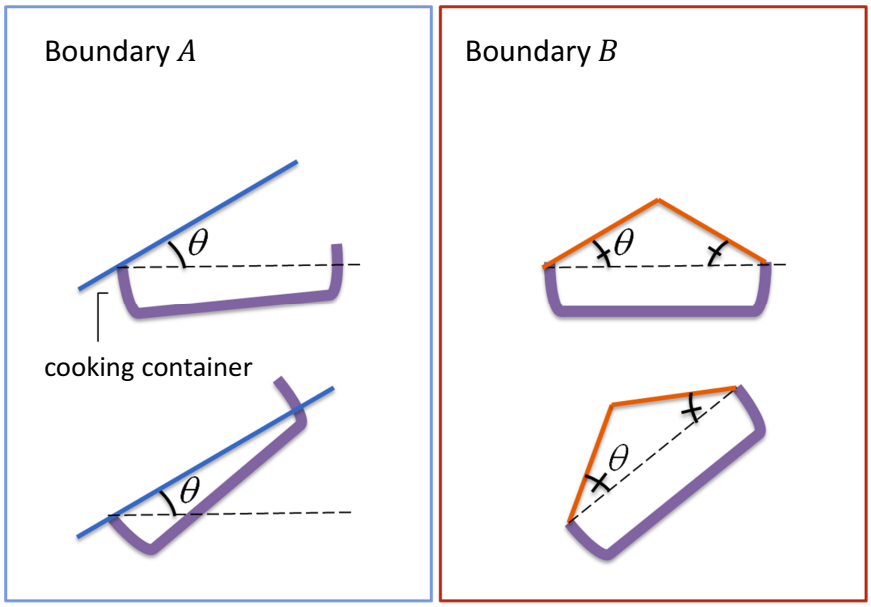

Fig. 14: Spill boundary of GIB

2-5. GIB collapse with TS

In this section, we consider collapse of a part of a GIB, and propose the model

which we use the Gauss function to define a TS for collapse. Sectional views of a typical image of a GIB before and after collapse are shown in Fig.15, 16. The difference between the two Gaussian surface is defined as the TS (Fig.17). A GIB which is piled up continues to collapse until it gets stable. Therefore, we assume the change of the piled up GIB during a certain time interval and use Gaussian surface as the piled up GIB with smooth slope.

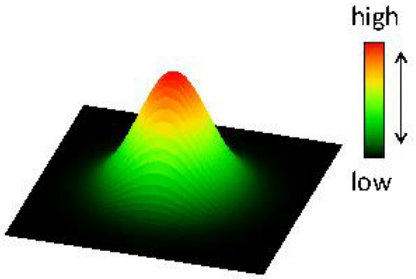

Fig. 15: Before collapse

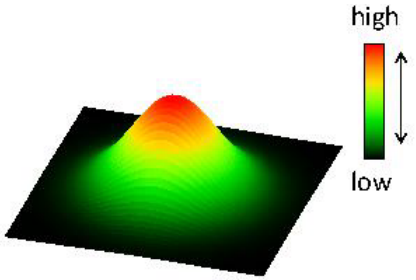

Fig. 16: After collapse

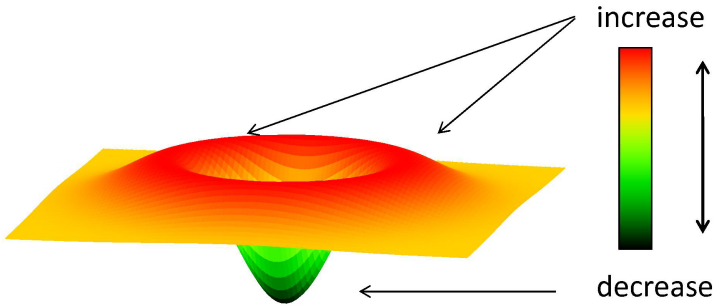

Fig. 17: TS of collapse

First, we find the areas where a part of a GIB may collapse and the center point of that area. We compare the height of an observe gird and adjacent grids to check the state of the piled up GIB locally. When an observe grid is the grid (x_i, y_j), we compare the height of the observe grid and four adjacent grids $h(x_{i-1}, y_j), h(x_{i+1}, y_j), h(x_i, y_{j-1}), h(x_i, y_{j+1})$ (Fig.18, 19, 20). If the height of the observe grid fulfills both following conditions,

$$h(x_i, y_j) > \frac{h(x_{i-1}, y_j) + h(x_{i+1}, y_j)}{2} \tag{10}$$

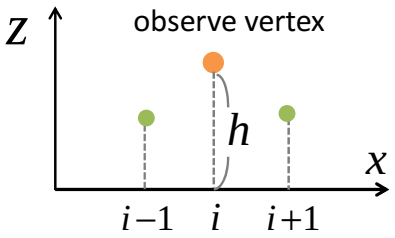

Fig. 18: Observe vertex

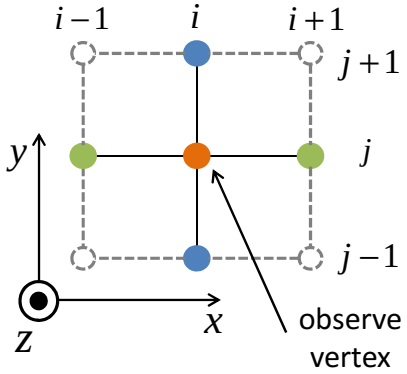

Fig. 19: Observe vertex and four adjacent grids vertex

$$h(x_i, y_j) > \frac{h(x_i, y_{j-1}) + h(x_i, y_{j+1})}{2} \tag{11}$$

we treat the grid(x_i, y_j) as a center point of the part of the GIB may collapse (Fig.20-4). We keep the top of the grid (x_i, y_j) as a candidate of a vertex for collapse. It is represented as a three-dimensional coordinate $(x_i, y_j, h(x_i, y_j))$. Moreover we consider a candidate of an area. It is a cone which has the vertex candidate as its apes (Fig.21). We treat collapse in it as one object. An angle of the conic slope of the area is an angle of repose which represents the angle that the GIB piled up keeps stability.

In the above process, a lot of area candidates are detected. If we calculate collapse of a part of a GIB in each area, calculation time increases. Thus we reduce vertex candidates using area candidates. For example, an area with a vertex candidate P includes other vertex candidate Q (Fig.22). In Fig.22, we assume that Q is included in the range of collapse centered at vertex P. We describe such collapse as the collapse at P. Calculation of collapse at Q is not considered and Q is removed from the vertex candidate list. For example, the top of the area candidate P and vertex candidates Q_1, Q_2 are shown in Fig.21. In Fig.21, Q_1 is removed from the vertex candidate. Candidate Q_2 is kept as the vertex candidate list because it is outside the cone. Vertex candidates are judged and reduced sequentially from the length vertex. After this process, we treat candidates in the vertex candidate list as a final vertex candidates (Fig.23).

We judge whether a part of a GIB collapses using area candidates based on the final vertex candidates. If a cone-shape GIB, for example, has the apex which is

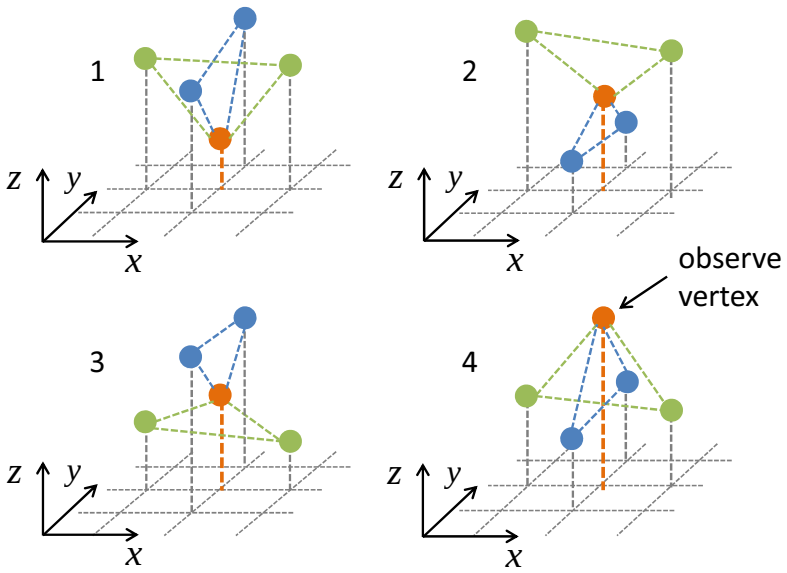

Fig. 20: Four conditions with observe vertex and adjacent grids vertex

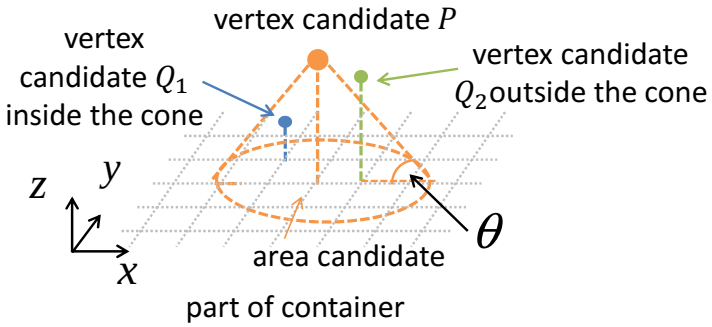

Fig. 21: Area candidate and vertex candidates

the same height of P, and has smaller volume than the volume of the cone with the apex P and the angle of repose θ, the angle of the GIB slope is larger than the θ. Although a shape of a GIB is of course different from a cone. we assume that the part of the GIB in the area collapses at P when the GIB volume is smaller than the reposed volume (Fig.24). The volume of the cone based on the area candidate with the final vertex candidate P is represented V_p, and the volume within the cone is represented V_{GIB} (the volume inside the dashed line in Fig.24). Both V_p and V_{GIB} are calculated as following.

$$V_p = \frac{(h(x_p, y_p))^3 tan^2\theta}{3} \tag{12}$$

$$V_{GIB} = \sum_{(x,y)\in C} \begin{cases} f(x_i, y_j) : f(x_i, y_j) < gen(x_i, y_j) \\ gen(x_i, y_j) : f(x_i, y_j) \geq gen(x_i, y_j) \end{cases} \tag{13}$$

Height from generatrix $gen(x_i, y_j)$ is the height of the perpendicular line from the generatrix to a bottom at the grid (x_i, y_j). Consequently $R = V_{GIB}/V_p < 1$, the

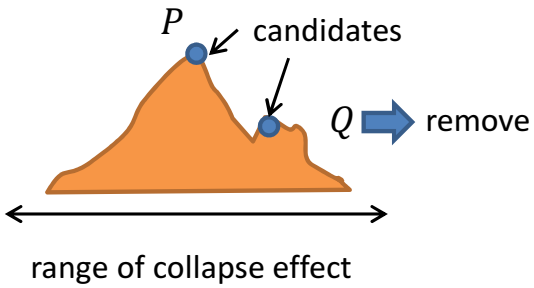

Fig. 22: Reduce Candidate

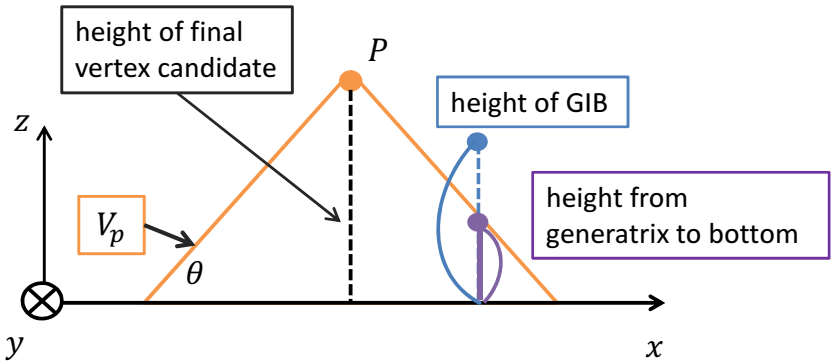

Fig. 23: Height of GIB, Generatrix and Final Vertex Candidate

part of the GIB should collapse. We apply a TS and the part of the GIB collapses. The central point G of the TS is matched with the final vertex candidate P. We can represent difference type of collapse with appropriate steps using the scaled TS according to the size of the collapse area.

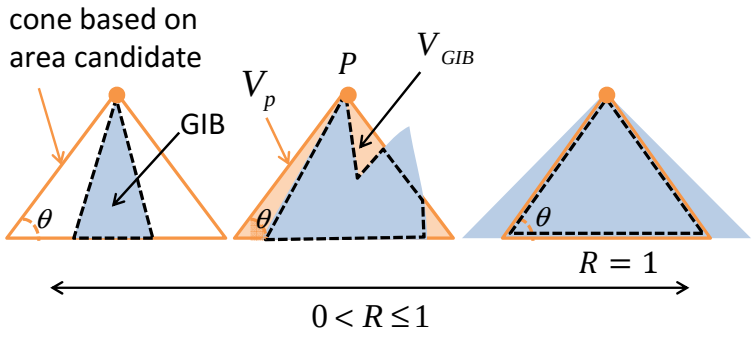

Fig. 24: Stability Judged with Angle of Repose and GIB Volume

3. MANIPULATION WITH COOKWARE

3-1. Push GIB manipulation

We have enabled to operate a GIB shaking and tilting a cooking container, however it is difficult to operate it directly. This subsection explains the model to operate GIB directly with rigid cookware. Although a frying pan is a kind of cookware, we call this as cooking container, and we define cookware is a kind of spatula.

In this model, we assumed that an operating surface of spatula is rigid and composed of one or more rectangles (we call it the operating surface). And in this first step, we also assumed that the operating surface is always vertical (a handle is upside). Then, we regard three-dimensional convex hull which is movement track of the operating surface (Fig.25), and we treat the interference of the convex hull and GIB as the one of the cookware and GIB.

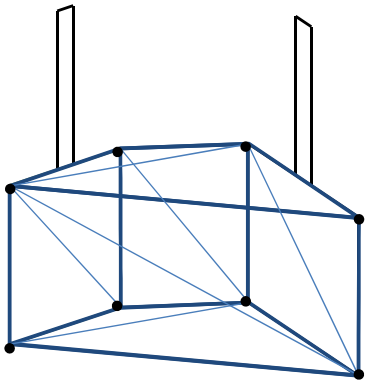

Fig. 25: Three-dimensional convex hull

Cookware move in three-dimensional space, so the vertices constituting the convex hull are represented by three-dimensional coordinate. When a height of GIB on the grid (x_i, y_j) is represented as $h(x_i, y_j)$, the point $(x_i, y_j, h(x_i, y_j))$ is defined as P^h_{ij}, and the point $(x_i, y_j, 0)$ is defined as P^z_{ij} identically. Then, if the following two conditions are satisfied, we judge the GIB interferes with the convex hull H_{ch}.

1. The convex hull H_{ch} is projected to H'_{ch} or thographically, then H'_{ch} and the grid P_{ij} satisfy $p_{ij} \subset H'_{ch}$.

2. The intersection P_{ij} of the convex hull H_{ch} and the straight line l_{zh} passing through P^z_{ij} and P^h_{ij} exists, then the distance of P^z_{ij} and P_{ij} is smaller than the value $h(x_i, y_j)$ of the height field grid.

We apply the affine transformation to the three vertices A_k, B_k and C_k of the triangle S_k that constitute the convex hull so that the straight line l_{zh} is vertical, and we determine these as A'_k, B'_k and C'_k (Fig.26). In addition, the straight line transformed to be vertical is l'_{zh}. If the intersection of the triangle S'_k and the straight line l'_{zh} is P'_{ijk}, the coordinate of P'_{ijk} is (x_i, y_j, z_{ijk}), and the value of P'^z_{ijk} is calculated as below.

$$P'^z_{ijk} = A'^z_k - \frac{1}{n'^z_k}\{n'^x_k(P'^x_{ijk} - A'^x_k) + n'^y_k(P'^y_{ijk} - A'^y_k)\} \tag{14}$$

Besieds, n'_k is the normal vector of the triangle S'_k.
When the convex hull interferes the straight, the lower height on the grid (x_i, y_j) is $h^{low}(x_i, y_j)$, and the higher one is $h^{high}(x_i, y_j)$ in order to distinguish two points (Fig.27).

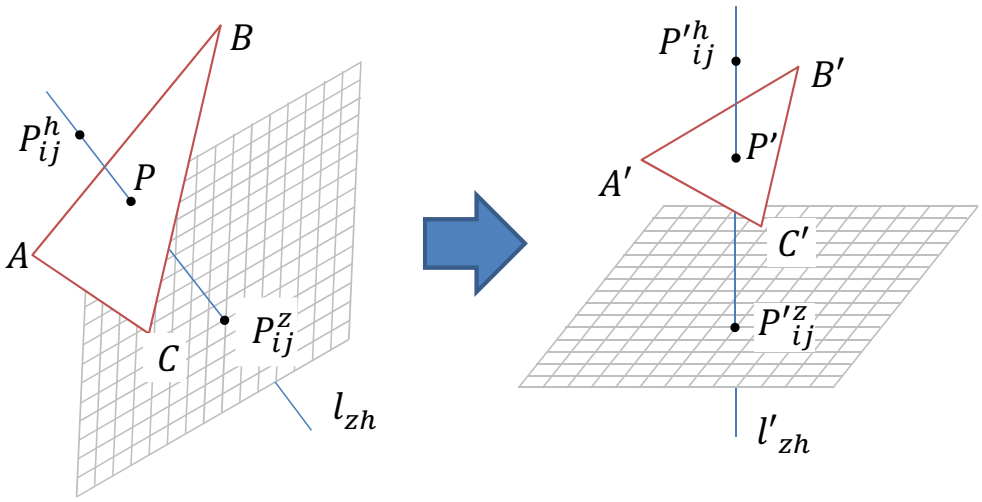

Fig. 26: Affine transformation

A part of the GIB that exists over the track of the operating surface is dragged by the friction (Fig.28). Then, if the operating surface interferes the grid (x_i, y_j), we determine the subtracted value v_{ij}^{sub} from the grid as below.

$$v_{ij}^{sub} = \begin{cases} 0 & (f(x_i,y_j) < h^{low}(x_i,y_j)) \\ f(x_i,y_j) - h^{low}(x_i,y_j) & (h^{low}(x_i,y_j) \le f(x_i,y_j) \\ & \le h^{high}(x_i,y_j)) \\ f(x_i,y_j) - (h^{high}(x_i,y_j) - h^{low}(x_i,y_j)) & \\ \quad - \dfrac{f(x_i,y_j) - h^{high}(x_i,y_j)}{2} & (f(x_i,y_j) > h^{high}(x_i.y_j)) \end{cases} \tag{15}$$

Therefore, the total subtracted volume V^{sub} is calculated using total number of grids N as follows.

$$V^{sub} = \sum^{N} v_{ij}^{sub} \tag{16}$$

By subtracting the volume V_{ij}^{sub} from the grid (x_i, y_j), we represent the GIB behavior which is transformed by the interference with the movement tracks of the operating surface.
In addition, the positive TS which is applied by the interference with GIB and cookware is a quarter of elliptic cylinder, and the parameters which define the TS is determined as below (Fig.29).

- Semi major axis of quarter elliptic cylinder a
- Semi minor axis of quarter elliptic cylinder b

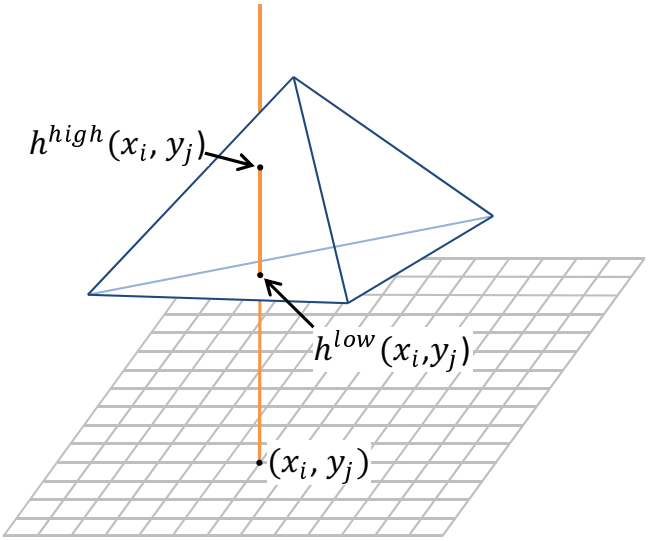

Fig. 27: Intersection of convex hull and straight line

- Width of quarter elliptic cylinder c
- Position in space o_C
- Straight line perpendicular to long and short axis of ellipse L_C

The position o_C is determined by the reference point set on the operating surface. The width of elliptic cylinder c is the one of the operating surface. The Straight line perpendicular to long and short axis of ellipse L_C is parallel with the normal line of the operating surface, and it obtains the point o_C. The semi major axis a is set to be parallel with the normal line of the operating surface, and the semi minor axis b is set to be parallel with it and perpendicular to the bottom of it. The semi major axis a is determined from moving speed of cookware v, normal line of the operating surface n, and constant T_3 as below.

$$a = T_3|v \cdot n| \tag{17}$$

The value to add the grid by this quarter elliptic cylinder is calculated from the total subtracted volume V^{sub}, so the semi minor axis b is a constant.

3-2. Press GIB manipulation

In our previous model, the operating surface of the cookware is always limited to the vertical, it can be expressed as 4DOF operation. At the second step described in this section, we assume that the operating surface of cookware is horizontal for simplifying discussion focus. If a GIB is pressed with cookware, it is assumed that the GIB around the operating surface is transformed. First of all, we judge the interference between GIB and cookware, and subtract the interfered area of GIB. Next, we represent the appearance of swelling of GIB around the operating

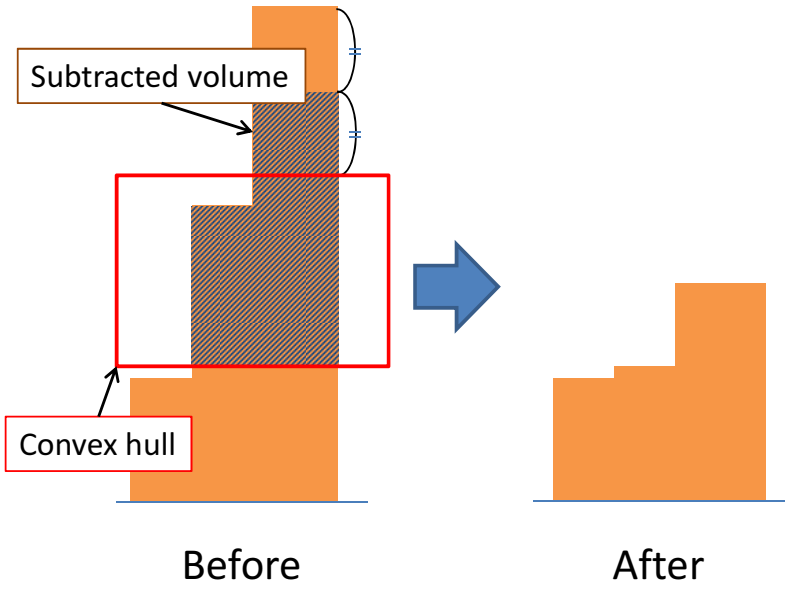

Fig. 28: Interference of convex hull and GIB

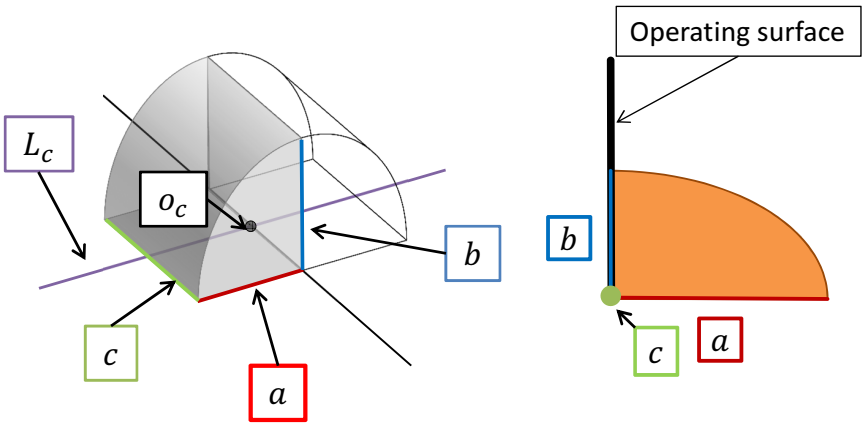

Fig. 29: Parameter of quarter elliptic cylinder

surface when a GIB is pressed with cookware with half-torus TS which a torus is divided into upper and lower. Furthermore, we represent more natural swelling of a GIB by changing the size and shape of half-torus according to the movement speed of cookware and the area that is pressed with cookware.
The parameters of the TS are defined as below (Fig.30).

- Large radius of torus R
- Small radius of torus r
- Position in container o_T

A GIB receives a force from the operating surface by pressing the GIB with cookware. At this time, we assume that the force depends on the position of the center

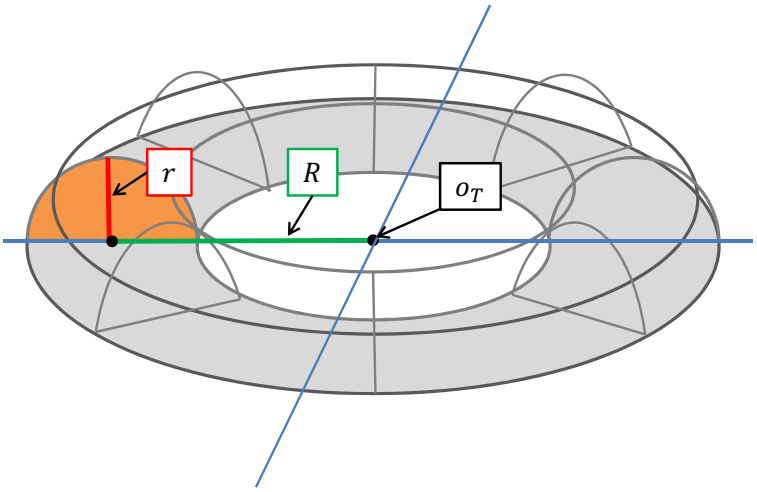

Fig. 30: Parameters of half-torus

of gravity G_T of the GIB which is pressed, and we define the position o_T of the TS is the center of gravity G_T. The position of the center of gravity G_T of GIB is calculated as below(Fig.31, 32).

$$G_T = \frac{1}{S_T} \sum^{N} m_{ij}^{'} \tag{18}$$

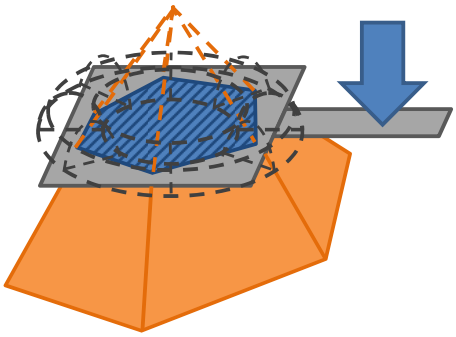

Fig. 31: Pressing GIB manipulation

Where S_T is the area of GIB which is pressed with cookware, N is the number of gird that the operating surface interferes, and $m_{ij}^{'}$ is the grid coordinate of the height field which is pressed. In addition, the large radius R of torus is calculated as below by approximating it as the radius of the circle that is same as the area S_T.

$$R = \sqrt{\frac{S_T}{\pi}} \tag{19}$$

The volume of half torus is calculated by the volume which is subtracted by the manipulation of pressing GIB. Therefore, the small radius r of torus is calculated as below by using the volume V^{sub} which is subtracted by the manipulation of pressing GIB, and the large radius R.

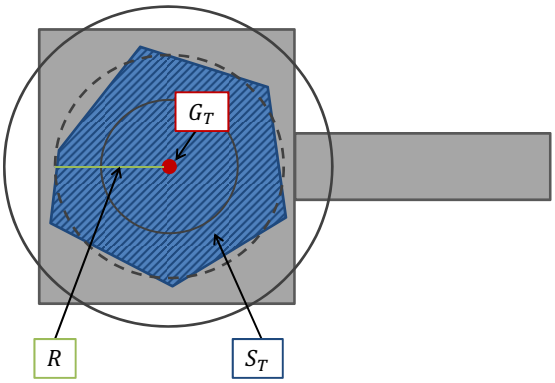

Fig. 32: Pressing GIB manipulation

$$r = \frac{1}{\pi}\sqrt{\frac{V^{sub}}{R}} \tag{20}$$

3-3. Scoop GIB manipulation

A GIB is divided into the part that remains in container and the part that moves on cookware when a GIB in container is scooped with cookware. Therefore, we define the height field on the operating surface of cookware. When the volume of the GIB on the cookware grid (x'_i, y'_j) is defined as $V'(x'_i, y'_j)$, the GIB volume V_{sp} on the cookware is calculated as below.

$$V_{sp} = \sum V'(x'_i, y'_j) \tag{21}$$

First of all, we consider the state that cookware interferes with a GIB by moving cookware horizontally (Fig.33). If we pull the cookware in the upper or horizontal direction, we move the part of GIB on the operating surface from the height field of container to the height field of cookware. The value v_{ij}^{move} of the grid which is moved from the cooking container to the cookware is calculated as below by the usual convex hull.

$$v_{ij}^{move} = \begin{cases} 0 & (f(x_i, y_j) < h^{low}(x_i, y_j)) \\ 0 & (h^{low}(x_i, y_j) \leq f(x_i, y_j) \leq h^{high}(x_i, y_j)) \\ f(x_i, y_j) - h^{high}(x_i, y_j) & (f(x_i, y_j) > h^{high}(x_i, y_j) \text{ and } v_{xy} < T_4) \\ \dfrac{f(x_i, y_j) - h^{high}(x_i, y_j)}{2} & (f(x_i, y_j) > h^{high}(x_i, y_j) \text{ and } v_{xy} \geq T_4) \end{cases} \tag{22}$$

By the way, v_{xy} is the movement velocity of a cookware in the plane xy, and T_4 is constant. Consequently, the total volume of a GIB which moves to the cookware V_{move} is calculated as following.

$$V^{move} = \sum v_{ij}^{move} \tag{23}$$

In addition, a GIB moves onto a cookware, the value v_{ij}^{sub} of grid is subtracted by the interference with the operating surface of a GIB and the total subtracted volume V^{sub} is changed as below.

$$v_{ij}^{sub} = \begin{cases} 0 & (f(x_i, y_j) < h^{low}(x_i, y_j)) \\ f(x_i, z_j) - h^{low}(x_i, z_j) & (f(x_i, y_j) \geq h^{low}(x_i, y_j)) \end{cases} \tag{24}$$

$$V^{sub} = \sum v_{ij}^{sub} - V^{move} \tag{25}$$

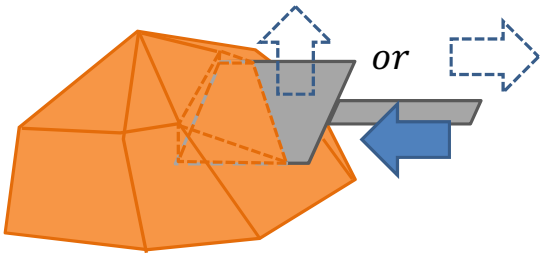

Fig. 33: Scooping GIB manipulation

We suppose that a GIB maintains the shape because the operating surface of a GIB is limited to horizontal, and we define the shape of the GIB on the operating surface as a cone experimentally (Fig.34). Because the situation is complicated by collapse of GIB both in container and on cookware. In this regard, we have been developing separately. In the first place, the center grid of the bottom of cone G_s is calculated by weighted average where each weight is each grid height of the operating surface respectively. We decide the radius of the bottom of cone r' to contact with the edge of the operating surface at least (Fig.35). In addition, the height of cone f_c to accord with the original volume V_{sp} is calculated as following.

$$f_c = \frac{3V_{sp}}{r'^2\pi} \tag{26}$$

If the angle between the bottom of cone and the bus ϕ is bigger than the angle of repose that we decided as θ previously, the radius of the bottom of cone r' and the height of cone f_c are changed as below so that this angle ϕ is equal to the angle of repose θ.

$$r' = \sqrt[3]{\frac{3V_{sp}}{\pi tan\theta}} \tag{27}$$

$$f_c = r' \cdot tan\theta \tag{28}$$

Besides, the center of the bottom of cone G_s is moved to the center of the operating surface, and the shape and position of cone is decided as we mentioned before. At this time, we limit the initial shape of GIB on the operating surface to a cone. However, we enable the simple manipulation of scooping GIB by this method, and we can sort out the problems to improve this model.

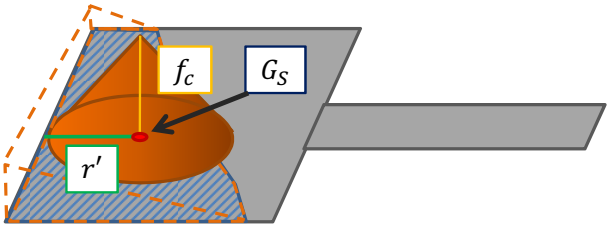

Fig. 34: Representation of scooping by cone TS

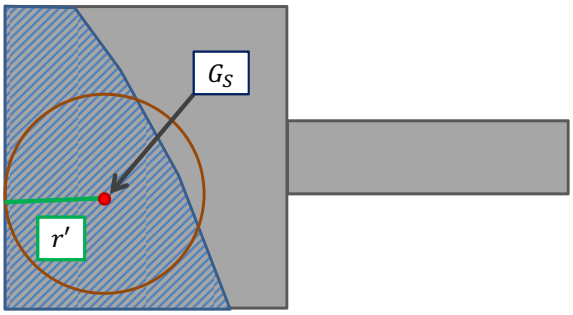

Fig. 35: Representation of scooping by cone TS

4. EXPERIMENT AND RESULT

We constructed the experimental system based on the proposed model with C++ language and DirectX. The specification of PC is the following; CPU: Intel Core i5-2400, 3.10GHz. The appearance of the experimental system is shown Fig.36. In this experimental system, we used the Wii remote released from Nintendo and the PATRIOT released from PLHEMUS as input devices. The GIB is assumed as fried rice, and the container is assumed as a frying pan. The GIB is drawn by the texture mapping. First, the appearance of tilting, shaking, tossing, spilling, and collapse GIB are shown in Fig.37, 38, 39, 40 and 41. Next, the appearance of pushing, pressing, and scooping GIB with a cookware are shown in Fig.42, 43 and 44. These figures show that lots of kind GIB operations are realized.

Fig. 36: Appearance of experiment system

Fig. 37: Appearance of tilting container

Fig. 38: Appearance of shaking container

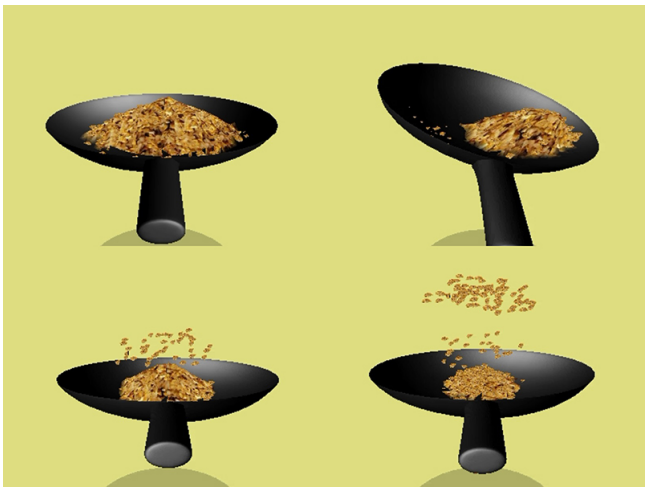

Fig. 39: Appearance of tossing GIB

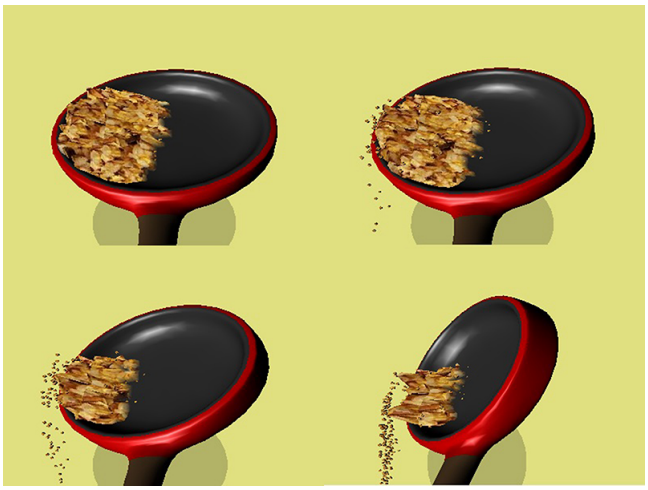

Fig. 40: Appearance of spilling GIB

Fig. 41: Appearance of collapse of GIB

Fig. 42: Appearance of pushing GIB

Fig. 43: Appearance of pressing GIB

Fig. 44: Appearance of scooping GIB

In addition, we evaluated the relationship between grid size of height field and processing speed in proposed model, actually without shake, toss and horizontal press with spatula manipulation because of pilot system. The processing speed of each grid size is shown in TABLE 1. We assumed that the bottom of the cooking container is a circle with a diameter of 32.5cm, and the operating surface of cookware is a square 100mm on a side. And we also adjusted the resolution of the container grid and the cookware grid. According to the result, processing speed of the experiment is much faster than the speed that is required for interactive manipulation (10∼12fps). However it is not excessive, because we have to implement toss and shake manipulation, and develop 6DOF spatula operation model. We also would like to consider about washing, cutting and dishing up procedures for a complete cooking learning system.

Next, several subjects used and evaluated the system. We set the gird size of height field is 16.5mm×16.5mm in the experimental system. According to the evaluation, we got positive opinions. Moreover, we got some opinions that the GIB behavior is natural and subjects felt to operate a cookware really.

TABLE 1: RESULT OF PERFORMANCE TEST

grid size [mm]	processing speed [fps]
16.5×16.5	721
12.5×12.5	496
9.5×9.5	286

5. CONCLUSION

We proposed an interactive manipulation model of a Group of Individual Bodies (GIB), and developed a cooking learning system as a VR-learning system. This model can calculate GIB behavior with high processing speed with Transform Surface (TS). Users can experience various manipulations, i.e., to move a group of small ingredients in a cooking container, toss and spill it. We also proposed the method how to calculate manipulations with spatula-formed cookware. Using our system you can learn cooking anytime, anywhere, even if you have no time to learn cooking because of busyness. As the experimental result shows, the proposed model can drive with high processing speed. This model can be applied to interactive manipulation systems.

However the operating surface of a spatula is always limited to vertical or horizontal, because this spatula manipulation as 6DOF operation is still difficult. As a future work, we have to develop the method to calculate 6DOF spatula manipulation, and realize actual spatula operation. Furthermore we will develop the models for other cooking processes such as washing and cutting ingredients and dishing them, then we would like to release the VR Cooking School system.

ACKNOWLEDGMENT

We thank our collegues in our laboratory for useful discussions. This work was supported in part by JSPS KAKENHI Grant Number 24501186.

REFERENCES

Nippon Housou Kyoukai, https://www.nhk-book.co.jp/recommend/80-02anni/gogaku/, (in Japanese)

Hilliard, R. L. and Keith, M. C. 2010. The Broadcast Century and Beyond: A Biography of American Broadcasting (5th edition), Focal Press.

Swan, K., Meskill, C. and Demaio, S. 1998. Social Learning from Broadcast Television (Media Education Culture Technology), Hampton Pr.

Garrison, D. R. 2011. E-Learning in the 21st Century: A Framework for Research and Practice, Routledge.

Marriott, R. D. C. V. and Torres, P. L. 2008. Handbook of Research on E-Learning Methodologies for Language Acquisition, Information Science Reference.

Ishihara, T. and Funahashi, K., Partial Sphere Container as Chinese Pan with Convex Bottom for Virtual Cooking System, *Proceedings of IWAIT 2013*, 957-962, 2013.

Kurimoto, Y. and Funahashi, K., The Collapse of Group of Individual Bodies Using Transformation Surface for Virtual Cooking System, *Proceedings of IWAIT 2013*, 118-123, 2013.

Natsume, Y., Lindroos, A., Itoh, H. and Funahashi, K., The Virtual Chemical Laboratory Using Particle and Volume Based Liquid Model, *Proceedings of SCIS & ISIS 2010*, 1354-1359, 2010.

Tanabashi, T., Itoh, H. and Funahashi, K., Representation of Wave Surface on Virtual Water Manipulation, *Proceedings of SCIS & ISIS 2008*, pp.1460-1465, 2008.

Miyashita, S. and Funahashi, K., Envelopment Surface Rendering of Falling Water for Particle and Volume Based Virtual Liquid Manipulation Model, *Proceeding of NICOGRAPH International 2011*, P02 (CD-ROM), 2011.

Miyashita, S. and Funahashi, K., Falling Water with Key Particle and Envelope Surface for Virtual Liquid Manipulation Model, *Proceeding of ACM VRST2012*, pp.197, 2012.

Funahashi, K. and Iwahori, Y., Manipulation of Liquid Using Cases in Virtual Space, *Proceeding of IEEE ROMAN2000*, pp.368-373, 2000.

Funahashi, K. and Iwahori, Y., Virtual Liquid Manipulation Using General Shape Vessel, *Proceeding of IEEE VR2001*, pp283-284, 2001.

Uchiyama, K. and Funahashi, K., Tablet VR-Learning System: Chemical Laboratory Experience System, *Proceeding of SITIS2013 (Workshop on CIS)*, pp.416-423, 2013.

Kato, F., Mitake,H. and Hasegawa,S., Interactive Cooking Simulator, In: *Proceedngs of the 15th Virtual Reality Society of Japan Annual Conference (academic lectures)*, 2D2-2 (DVD-ROM), 2010. (in Japanese)

Stora, D., Agliati, P. O., Cani, M. P., Neyret, F. and Gascuel, J.D. 1999. Animating Lava Flows, Graphics Interface '99, pp.203-210.

Onoue, K. and Nishita, T., Virtual Sandbox, In: *Proceedings of the 11th Pacific Graphics*, pp.252-259, 2003.

Morii, A., Yamamoto, D. and Funahashi, K., Interactive Manipulation Model of Group of Individual Bodies for VR Cooking System, *Proceedings of ICEC2010*, pp.484-486, 2010.

Morii, A., Kamigaito, S., Yamamoto, D. and Funahashi, K. 2011. Existence Probability Particle Based Interaction Model of Group of Individual Bodies for VR Cooking System, Transactions of the Virtual Reality Society of Japan, Vol.16, No.4, pp.539-549. (in Japanese)